

Electron energy-loss spectroscopy analysis of interface structure of yttrium oxide gate dielectrics on silicon

D. Niu and R. W. Ashcraft

Department of Chemical Engineering, North Carolina State University, Raleigh, North Carolina 27695

Z. Chen and S. Stemmer

Department of Mechanical Engineering and Materials Science, Rice University, Houston, Texas 70005

G. N. Parsons^{a)}

Department of Chemical Engineering, North Carolina State University, Raleigh, North Carolina 27695

(Received 18 March 2002; accepted for publication 29 May 2002)

Interface stability of high dielectric constant gate insulators on silicon is an important issue for advanced gate stack engineering. In this article, we analyze the silicon/dielectric interface structure for thin Y_2O_3 and Y silicate films deposited by chemical vapor deposition on clean and prenitrided Si(100) using high-resolution transmission electron microscopy, electron energy-loss spectroscopy, and x-ray photoelectron spectroscopy. The analysis shows the films to be stoichiometric Y_2O_3 on top and Y-silicate/ SiO_2 at the dielectric/Si interface. Pre-nitridation of the silicon surface impedes the reaction between the depositing film and the substrate, promoting a Si-free Y_2O_3 structure. Possible mechanisms leading to the observed Y_2O_3 and Y silicate structures are discussed. © 2002 American Institute of Physics. [DOI: 10.1063/1.1496138]

The International Technology Roadmap for Semiconductors has called for the equivalent of a sub-1 nm silicon dioxide gate dielectric.¹ The leakage current of pure SiO_2 at 1 nm would be unacceptably high, leading to problems in reliability and heat generation. High dielectric constant (high- k) materials enable larger film thicknesses for the same gate capacitance, and therefore lower leakage current. One of the important issues to be addressed with high- k dielectrics is the stability of the high- k /silicon interface. Several metal oxides that are potentially stable in contact with silicon are under investigation,^{2–6} including Al_2O_3 , Y_2O_3 , La_2O_3 , HfO_2 , and ZrO_2 . Metal silicates, such as Zr, Hf, and Y, have also attracted attention.^{7,8} Many research groups have reported interface reactions with the silicon substrate during deposition or postdeposition anneals that lead to mixed metal/oxygen/silicon layers at the interface. The mixed layers have a smaller k than the deposited dielectric, reducing the net dielectric constant of the insulating layer. In this article, we analyze the interface structures of thin Y_2O_3 and Y silicate on Si(100) deposited by chemical vapor deposition (CVD) using x-ray photoelectron spectroscopy (XPS), high-resolution transmission electron microscopy (HRTEM), and electron energy-loss spectroscopy (EELS), and use the sub-nanometer resolution to gain insight into mechanisms associated with dielectric/substrate reactions during deposition.

Thin Y_2O_3 films were deposited by oxygen plasma assisted CVD using tris(2,2,6,6-tetramethyl-3,5-heptanedionato)yttrium [$Y(TMHD)_3$] introduced downstream from an O_2 plasma. The substrate temperature was fixed in the range of 350 °C to 450 °C. Substrates of 0.1–0.3 $\Omega \cdot cm$ p -type Si(100) were cleaned with a JTB-100 baker clean solution and dipped in 10:1 buffered HF solution be-

fore being immediately transferred to the loadlock chamber. Details of the operation conditions and sample preparation are presented elsewhere.⁹ XPS was performed on a Riber LAS 3000 with a MAC2 analyzer using nonmonochromatic Mg $K\alpha$ x rays (1253.6 eV). Scanning transmission electron microscopy EELS data was collected using a JEOL JEM 2010F 200 kV transmission electron microscope equipped with a field-emission gun, an annular dark-field (ADF) detector, and a Gatan GIF200 postcolumn imaging filter,¹⁰ capable of achieving of sub-0.2 nm probe sizes for microanalysis and incoherent Z-contrast lattice imaging.

Figure 1 shows the XPS Y 3d spectra for films deposited at 400 °C for 3, 6.5, and 30 min with thicknesses of approximately 65 Å and 100 Å [determined from transmission electron microscopy (TEM)], and ~500 Å (determined from step-height profilometry), respectively. Each film in Fig. 1 was annealed *ex situ* at 900 °C in N_2 ambient (with $>10^{-5}$ Torr O_2) for 1 min. XPS analysis of the thickest film shows features consistent with Y_2O_3 in the Y 3d spectrum at 156.8 and 158.8 eV ($3d_{5/2}$ and $3d_{3/2}$).¹¹ For the thinner films, the Y 3d peaks are shifted to higher binding energies, consistent with an oxide structure that contains significant Y—O—Si

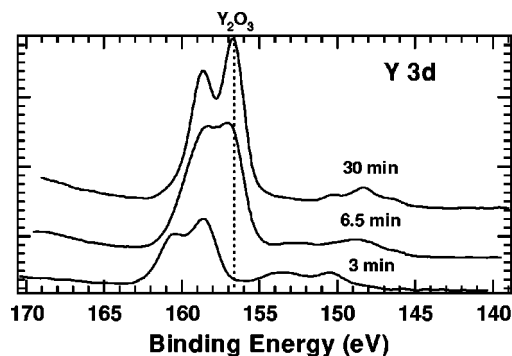


FIG. 1. XPS Y 3d spectra of CVD " Y_2O_3 " films with various thicknesses.

^{a)} Author to whom correspondence should be addressed; electronic mail: gnp@ncsu.edu

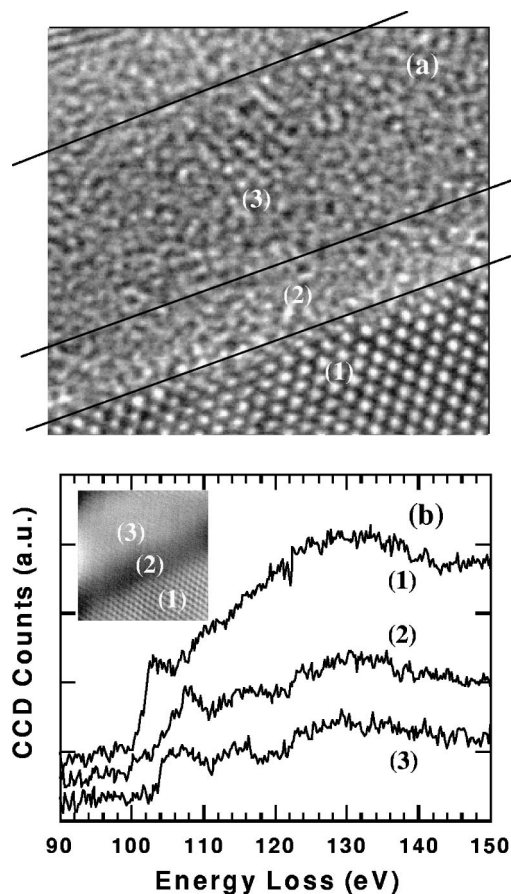


FIG. 2. (a) TEM of the film deposited at 400 °C for 3 min and annealed at 900 °C for 1 min. The thickness is about 65 Å; (b) Si *L* edges measured across the film. The locations correspond to those on the TEM image.

(Y-silicate) bonding. For the 100 Å film, the peak positions are between the peaks for the other samples, consistent with a multiple-layer structure. The Si 2*p* spectra for the 500 Å film shows no evidence for silicon in the top 50–75 Å of the film (i.e., the thickness probed by XPS),⁹ but a Si—O peak at 102.5 eV is observed in the 65 Å film, consistent with Y-silicate bonding.

Figure 2 shows (a) HRTEM and (b) EELS results of a film deposited under the same conditions as the 65 Å film shown in Fig. 1. ADF imaging was used to position a ~0.2 nm probe for EELS of the Si *L* edge for compositional analysis through the film thickness. The Si *L*-edge data in Fig. 2 is offset for clarity. The inset of Fig. 2(b) shows the ADF image. Region 1 is the silicon substrate with an edge onset at 99 eV and clear periodic fringes in the TEM. Region 2 is dark in the ADF with the edge onset shifted to a higher-energy loss (105 eV). Also, the EELS near-edge fine structure shows peaks near 106, 108, and 115–116 eV, similar to SiO₂. The TEM image indicates the thickness of region 2 is about 2.0 nm, and the yttrium concentration in region 2 is below the detection limit of the method. However, EELS is less sensitive to Y than to Si, and we can not rule out the possibility of some yttrium in region 2. Region 3 is lighter in ADF, consistent with an increased concentration of the heavier element (yttrium). Si *L*-edge onset in region 3 is approximately 104 eV, with another feature at ~116 eV, consistent with yttrium silicate. HRTEM analysis of a 100 Å film, deposited under the same conditions as the 100 Å film

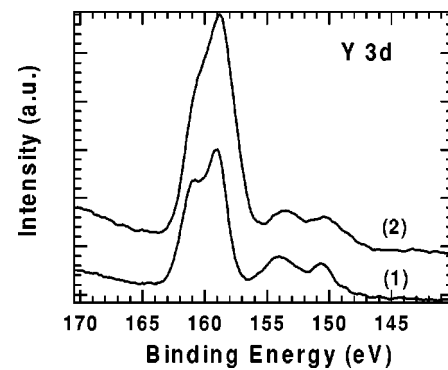


FIG. 3. XPS Y 3*d* spectra of CVD “Y₂O₃” films on (1) bare Si and (2) nitrided Si.

in Fig. 1, shows a clear double-layer structure, with a crystalline layer on top and an amorphous layer at the interface, consistent with the XPS results.

The effects of substrate pretreatments were also investigated. Figure 3 shows the Y 3*d* spectra of thin films deposited for 1 min on (1) clean Si and (2) nitrided Si, respectively. The nitridation was performed *in situ* at 400 °C by exposing the clean silicon surface to a N₂ plasma for 20 min prior to Y₂O₃ deposition. This plasma pretreatment leads to approximately one monolayer of N at the Si/dielectric interface.¹² After dielectric deposition the films were annealed *ex situ* at 900 °C in N₂ for 10 min. For the film deposited on nitrided Si (spectrum 2), the Y 3*d*_{5/2} peak appears at a slightly lower binding energy than that for the film deposited on clean Si. The peak positions in both films are shifted higher relative to Y₂O₃ (156.8 eV), consistent with a Y—O—Si structure, with a larger Y/Si ratio (i.e., less interface reaction) in the films deposited on the nitrided silicon. The Si 2*p* and O 1*s* spectra also show consistent results.⁹

Figure 4 shows results of TEM/EELS analysis for a 70 Å film deposited on nitrided silicon. The film was annealed in N₂ at 900 °C for 1 min before analysis. HRTEM results in Fig. 4(a) suggest three regions in the film. The top layer (region 4) is partially crystallized, while the bottom layers (region 2 and 3) remain amorphous. The EELS data was acquired at ~1 nm (region 2), ~2.3 nm (region 3), and ~5.5 nm (region 4) from the substrate. The Si *L*-edge curves are again offset for clarity. For region 2, the EELS data shows an onset edge of 105 eV and peaks near 106, 108, and 115–116 eV, consistent with a SiO₂-like layer. For region 3, Si peaks are still observed but with reduced intensity as compared to region 2, consistent with a Y—O—Si structure. In region 4, no silicon features are observed in the EELS data, consistent with a Y₂O₃ structure.

Two distinct issues need to be addressed to more fully understand interface reactions during high-*k* deposition and postdeposition processing: (1) SiO₂ formation at the silicon/dielectric interface; and (2) reactions between the dielectric and the substrate that lead to mixed metal/oxygen/silicon (silicate) layers. The data presented herein indicate that for the case of Y₂O₃ deposition on silicon, both SiO₂ and silicate layers can form near the interface.

Several possible routes exist for introduction of excess oxygen into the interface reaction zone. One possibility is diffusion of residual oxygen present during annealing

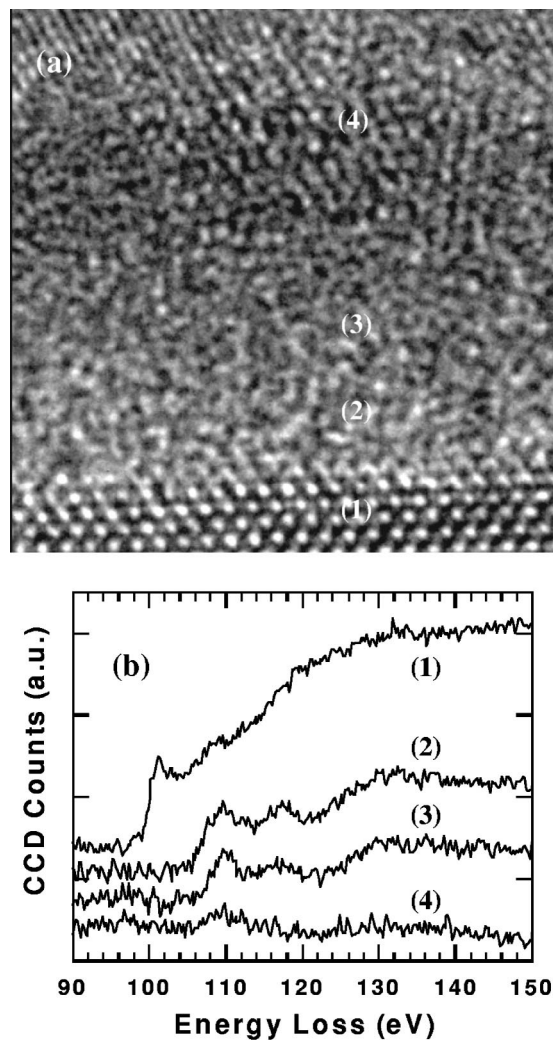


FIG. 4. (a) TEM of Y_2O_3 on nitrided Si, (b) Si L edges of the same film: (1) Si bulk, (2) 1 nm from Si interface, (3) 2.3 nm from Si interface, and (4) 5.5 nm from Si interface.

through the high- k layer, and another possibility is hydroxides, produced during deposition or introduced by postdeposition absorption from the ambient.¹³ Recent results of Y-silicate films that were capped *in situ* with poly-Si before annealing indicate that interfacial SiO_2 is significantly reduced (<0.5 nm) as compared to uncapped films (~ 2 nm observed here),¹⁴ consistent with significant oxidation resulting from O_2 diffusion or H_2O absorption.

Regarding the formation of the Y—O—Si layer, it is likely that diffusion of Si through the interface layer plays an important role, although metal diffusion may also occur. The importance of silicon diffusion is consistent with the result of the N_2 pretreatment studies. The presence of interface nitrogen leads to films with a larger Y/Si ratio, and promotes formation of Y_2O_3 films. This is consistent with interface N decreasing the rate of Si diffusion from the substrate into the deposited dielectric.

It is important to note that the ~ 2 nm interfacial SiO_2 is observed for uncapped films after exposure to atmosphere. Using *in situ* poly-Si capping layers, interfacial layers less than 0.5 nm have been achieved, so we expect that the approaches to control interface composition reported here (*in situ* capping and substrate pretreatment) will allow equivalent oxide thicknesses (EOTs) to scale to 1.0 nm. In the 1 nm EOT regime, the surface prenitridation process presented will reduce the rate of interface silicate formation, but silicate formation mechanisms will still be active.

Ideally, one would like to know the mechanisms that govern silicon diffusion and how it can be controlled. With the data presented here, two limiting possibilities can be described. One possibility is that the extent of silicon intermixing is determined by the rate of silicon diffusion through the amorphous interface layer, and crystallization proceeds in the region where Si concentration is sufficiently low. A second possibility is that the extent of silicon diffusion is determined by the rate of Y_2O_3 crystallization, where silicon interdiffusion and reaction with the crystalline Y_2O_3 layer is slow. Unfortunately, there is not yet sufficient data to distinguish these two processes and determine the rate-limiting step in the interface reaction process. Understanding these reactions in more detail will be important to tailor silicon gate stacks for advanced device structures.

The authors appreciate the funding from SRC/SEMATECH Center for Front End Processes and NSF Grant No. CTS-0072784. One of the authors (S.S.) gratefully acknowledges the use of the STEM facilities at the RRC at the University of Illinois at Chicago (NSF DMR-960172).

¹S. I. Association, *The International Technology Roadmap for Semiconductors, 2001 edition* (S. I. Association, Austin, TX, 2001).

²L. Manchanda, W. H. Lee, J. E. Bower, F. H. Baumann, W. L. Brown, C. J. Case, R. C. Keller, Y. O. Kim, E. J. Laskowski, M. D. Morris, R. L. Opila, P. J. Silverman, T. W. Sorsch, and G. R. Weber, Tech. Dig. - Int. Electron Devices Meet. **1998**, 605 (1998).

³M. Gurvitch, L. Manchanda, and J. M. Gibson, Appl. Phys. Lett. **51**, 919 (1987).

⁴J. Shappir, A. Anis, and I. Pinsky, IEEE Trans. Electron Devices **33**, 442 (1986).

⁵M. Copel, M. Gribelyuk, and E. Gusev, Appl. Phys. Lett. **76**, 436 (2000).

⁶J. P. Maria, D. Wicaksana, A. I. Kingon, B. Busch, H. Schulte, E. Garfunkel, and T. Gustafsson, J. Appl. Phys. **90**, 3476 (2001).

⁷G. D. Wilk, R. M. Wallace, and J. M. Anthony, J. Appl. Phys. **87**, 484 (2000).

⁸J. J. Chambers and G. N. Parsons, J. Appl. Phys. **90**, 918 (2001).

⁹D. Niu, R. W. Ashcraft, Z. Chen, S. Stemmer, and G. N. Parsons (unpublished).

¹⁰E. M. James, N. D. Browning, A. W. Nicholls, M. Kawasaki, Y. Xin, and S. Stemmer, J. Electron Microsc. **47**, 561 (1998).

¹¹J. F. Moulder, W. F. Stickle, P. E. Sobol, and K. D. Bomben, *Handbook of X-ray Photoelectron Spectroscopy* (Perkin-Elmer, Eden Prairie, MN, 1992).

¹²J. J. Chambers and G. N. Parsons, Appl. Phys. Lett. **77**, 2385 (2000).

¹³D. Niu, R. W. Ashcraft, and G. N. Parsons, Appl. Phys. Lett. **80**, 3575 (2002).

¹⁴S. Stemmer, D. Klenov, Z. Chen, D. Niu, R. W. Ashcraft, and G. N. Parsons (unpublished).